A SMART CURRENT AND VOLTAGE ACQUISITION SYSTEM WITH HIGH ACCURACY FOR EV APPLICATIONS

Dai Haifeng, Zhang Xiaolong
Clean Energy Automotive Engineering Center, School of Automotive Studies
Tongji University, Shanghai 201804, China
Emails: tongjidai@gmail.com

Submitted: Aug.5, 2012 ***Accepted: Sep.7, 2012*** ***Published: Dec.1, 2012***

Abstract- Energy management is one of the most important tasks of the electric vehicles (EV) and is totally different with the management in the traditional internal combustion vehicles (ICV). To implement a pleasing management, the system should know the working current and terminal voltage of the traction battery systems very accurately. This paper presents a design of a smart current and voltage acquisition system with high accuracy for EV applications. The detailed structure and components, the simulation and error analysis of the system are introduced. And to enhance the accuracy, a smart error correction is designed as well. Several tests are applied to evaluate the proposed system, and testing results indicate a good performance of the system, the maximum current error is less than 0.05A and the maximum voltage error is less than 0.02V.

Index terms*:* Electric vehicles, current and voltage acquisition, simulation and analysis, error correction.

I. INTRODUCTION

Nowadays, due to the considerations on energy saving and environment protection, electric vehicles (EV), including hybrid electric vehicles (HEV), battery-powered electric vehicles (BEV) and plug-in hybrid electric vehicles (PHEV), have drawn more and more attention from the automotive companies from all over the world.

One of the very different tasks of the development of EVs, comparing with the traditional inner combustion vehicles, is the energy management system, which takes charge of the power coordinating between the driving system and the electric power supplies. To implement a pleasing management, the system should acquire the working current and terminal voltage of the traction battery systems very accurately [1-4]. The accuracy of the voltage and current measurements affects several aspects of the energy management, and one of the most critical parts is the SOC calculation of the traction battery. The SOC calculation, sometimes also called SOC estimation or prediction, plays a vital role in the energy management strategies. The accuracy of the SOC estimation is highly dependent on the model, algorithm and the current/voltage measurement [5-7]. Normally, with a poor current/voltage sampling, the accuracy of SOC estimation is poor. So, to enhance the performance of the electric vehicles, and meanwhile, improve the energy efficiency of the future electric transportations, a high accurate voltage and current acquisition system is very necessary [8].

The voltage measurement can be implemented by measuring the voltage on the direct current (DC) bus of the powertrain system, and by a voltage HALL sensor as well [9]. The voltage HALL sensor is proved to be with worse accuracy, high cost, so it is not very common in the EV applications. Direct voltage measurement on the powertrain DC bus also faces some difficulties anyway. The first one is that the voltage on the DC bus is very high, and normally higher than 100V, which is much higher than the voltage a general electronic system can bear. The second one is that the voltage on the DC bus is contaminated with a lot of noises. This is generally caused by the PWM operations from the motor controller. The noises are sometimes very remarkable comparing with the real bus voltage. These two obstacles make the voltage measurement hard to get a high performance, and some efforts should be made to achieve the high accurate measurement.

The current of the DC bus ranges generally from -400A to 400A. Thus the first difficulty in current measurement is that how to design a system accommodating such a wide measuring range. The measurement accuracy of the DC current should be always accurate over the whole range, it is really a challenge especially when the real current value is very low, say less than 10 A. Another aspect which should be also taken into account is that the current signal is normally contaminated by a lot of noise as well. Current measurement can be implemented with either a current HALL sensor or an accurate shunt resistor [9-17]. The shunt resistor can be designed and manufactured with high accuracy, and very low temperature shifting factor. Several applications are developed based on shunt resistors. However, the signal processing system is very complex for the high common voltage and very weak signal amplitude. Another drawback of the shunt resistor based system is that the system is founded on the high voltage framework, thus, for safety considerations, the signal should be isolated, which increases the cost and reduces the real performance. The HALL sensor, on the other hand, is an isolated measurement method. Although the accuracy is not as high as the shunt resistor systems, it could meet the requirements of the vehicular applications. The signal processing parts of the systems based on HALL sensor is simpler comparing with the shunt resistor based systems. Meanwhile, several productions of the HALL sensor are now available on the market, which speed up the development processes. The cost of the whole measurement system based on the HALL sensor is almost the same with the system based on the shunt resistors, although the HALL sensor is more expensive than shunt resistors, the price of the signal processing part is much lower than the shunt resistor based ones.

This paper studies a current and voltage acquisition system with high accuracy, and is immunity to the noise on DC bus. The current measurement is designed based on a HALL current sensor, while the voltage measurement is designed based on the idea of direct measuring the voltage on DC bus. The detailed structure of the system is described, and the system is simulated with pSpice to analyze the performance and characteristics. The error analysis and the noise correction of the system are also discussed. Several validation testing are implemented, and testing results indicate that the system proposed has a good performance and very suitable for EV applications.

The remainder of the paper is organized as follows. The structure and main components of the system is introduced in Section II. An analysis of the system by pSpice simulation is illustrated in Section III. The error analysis and error correction is discussed in Section IV. And the validation testing is demonstrated in Section V. Section VI gives out some primary conclusions.

II. STRUCTURE OF THE ACQUISITION SYSTEM

a. System architecture

The basic structure of the acquisition system is shown in Figure1. The system is composed of several parts: the current signal processing and conversion part, the voltage signal processing and conversion part, the HALL current sensor, the micro-controller unit (MCU), and the monitoring interface. The system can be configured to exchange data with the external unit with a CAN communication, a RS 232 communication or a PWM signal. The monitoring interface can either be connected with a monitoring PC or a higher-level ECU (electronic control unit), e.g., the vehicle controlling unit (VCU). Meanwhile the CAN communications can also be used as the configuration port, by which the functions and parameters of the system can be adapted according to applications. The power supply module is designed to provide the power supply needed by other modules. The MCU used in this system is a 16-bit processor MC9S12DP256, with a lot of configurable peripherals.

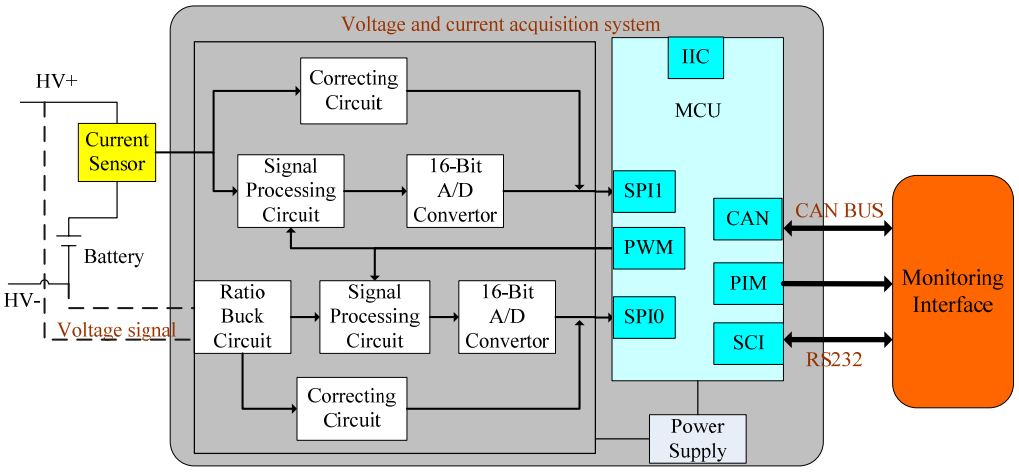

Figure 1. Structure of the acquisition system

b. The current measurement module

The current signal is firstly converted to a voltage signal ranging from -5V to 5V with a HALL current sensor produced by LEM. This sensor is a loop-closed, high accurate HALL sensor, with the conversion coefficient 2000:1, the measurement range is -450A to 450A, the accuracy is 0.05%, and linear degree is 0.001%. Signal bandwidth of the sensor is 100K, which is fully qualified for EV applications.

Since the output of the current sensor (com1 in Figure 2) is directional, a rectifier circuit should be employed to convert the signals into 0V to 5V range. The schematic of this part is illustrated in Figure 2(a), which is an absolute value circuit. The signal from the HALL sensor is firstly rectified with no attenuation. When input signal is positive, the circuit works just like a follower, while the signal is negative, the inverting circuit works to make the signal positive. The two diodes D301 and D305 are located in the feedback circuits, however, the forward voltage drops are almost eliminated of the operator. The D300 and D304 are used to prevent the operator OP301A and OP301B working in the saturated mode. This module works with a ±15V power supply. The direction of the current is judged with the circuit shown in Figure 2(b), which is actually a comparator.

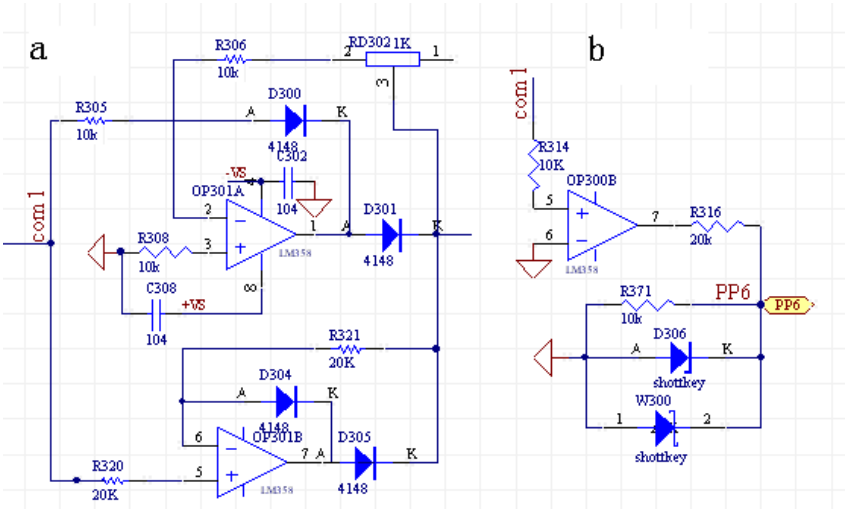

Figure 2. Schematic of the current measurement module

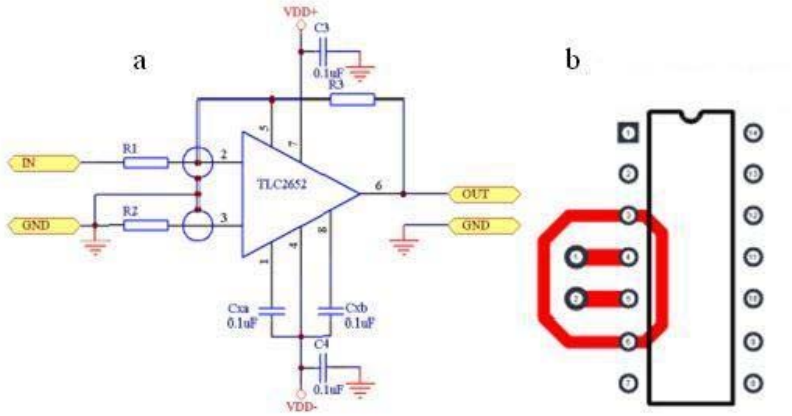

Figure 3. Schematic of the voltage measurement module

c. The voltage measurement module

The high voltage on the DC bus is firstly modulated to a voltage signal ranging from 0V to 5V with a differential circuit, as shown in Figure 3(a). When designing the PCB, to weaken the effect of leakage current, a protection circle is employed around the corresponding pins (Figure 3(b)). Both the converted voltage and current signals are then going through a filtering part composed of switch capacitor filter to filter the interference with high frequency, and enhance the signal to noise ration (SNR). A 5 order low-pass filtering is designed in the switch capacitor filter, and the cutoff frequency can be adjusted with the PWM coming from MCU. The filtered signals are at last input to a 16-bit AD converter. The A/D converter communicates with the MCU through SPI.

d. The power supply module

In the EV applications, the low-voltage power source is generally 12 V. In this system, the power supplies ±5V and ±15V are needed. Thus a DC/DC converter is used to provide the necessary power supplies. A good EMI design is also considered to weaken the affect caused by the fluctuations of power supply voltages.

III. ANALYSIS OF THE SYSTEM WITH PSPICE SIMULATION

a. Simulation and analysis of the current measurement module

Figure 4 shows the simulation schematic of the module. In the simulation, the power supply is set as an ideal power source, and the parameters of the ICs are set with those given out by the manufacturers.

A scanning simulation is implemented on the resistors used in the amplifying circuit and absolute value circuit. The resistor is named rval, and the scanning range is set from 10Ω to 1MΩ. Simulation result is illustrated in Figure 5. From Figure 5, we can find that, in the low frequency parts, the responds are almost the same when rval is 10kΩ, 100kΩ and 1MΩ.

The DC output characteristic is simulated, and the results are “V (OUT)/V(IN) = 4.997E+00, INPUT RESISTANCE AT V_V(IN) = 9.561E+11, and OUTPUT RESISTANCE AT V (OUT) = 1.000E+03”. Thus the theoretical DC sampling error is 0.06%. The AC simulation result is shown in Fig.6, which indicates that the bandwidth is about 1kHz.

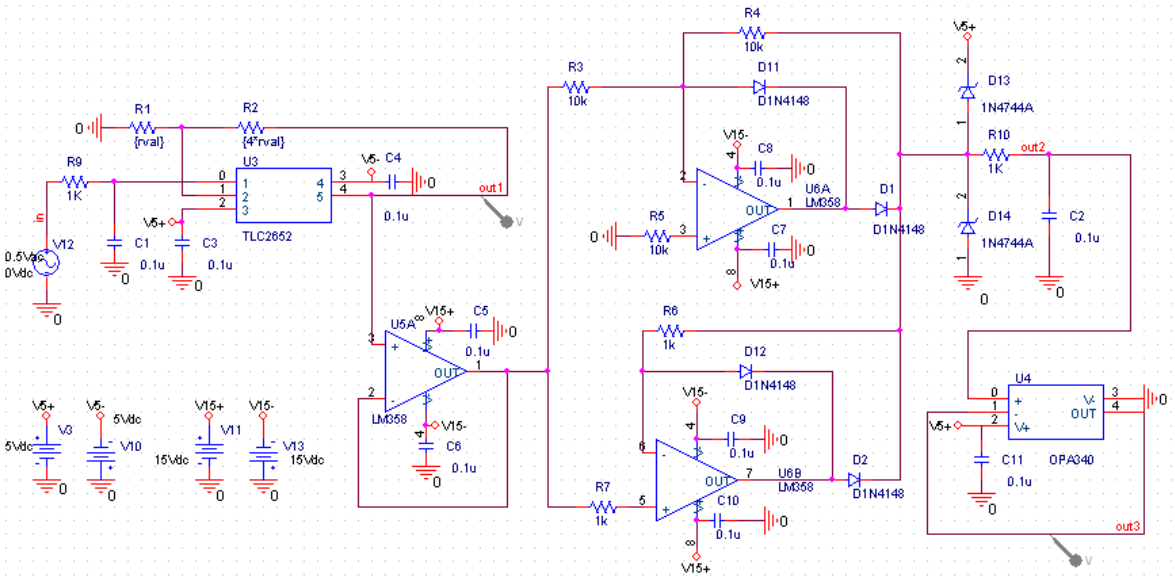

Figure 4. Simulation schematic of the current measurement module

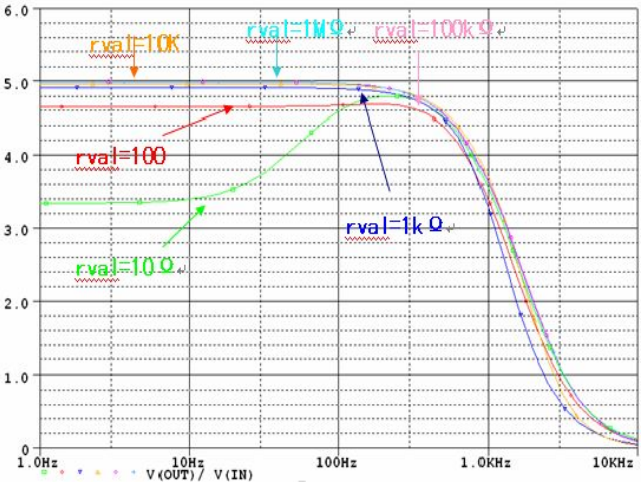

Figure 5. Frequency response with different resistors of the current measurement module

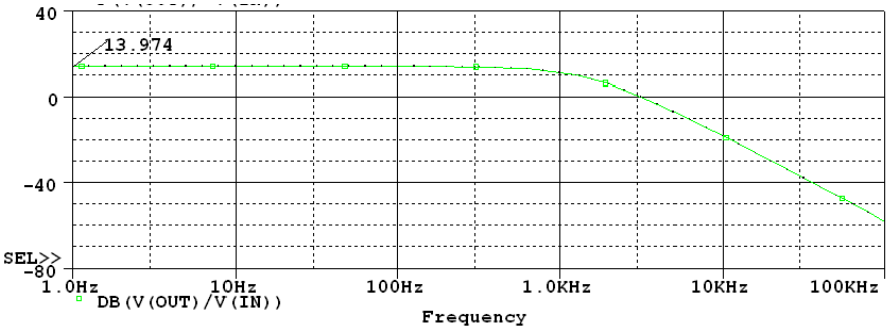

Figure 6. Simulation results of AC characteristics of the current measurement module

The transient response simulation result under the setups of that the initial voltage is 0V, pulse voltage amplitude is 0.5V, pulse period is 2ms, delay time is 0.99ms, dropping time is 0.01ms, and uprising time is 0.01ms is shown in Figure 7, which indicates a quick response on the pulse excitation.

The performance of the module working under different temperatures is also analyzed with simulation. The simulated temperatures include -20℃, 0℃, 25℃, 50℃ and 70℃. The simulated frequency responses are drawn in Figure 8. From Figure 8, the performance of the module is affected by high temperatures. However, considering the working condition of the real systems, the high temperature rarely exists, so the system can meet the requirements of real applications.

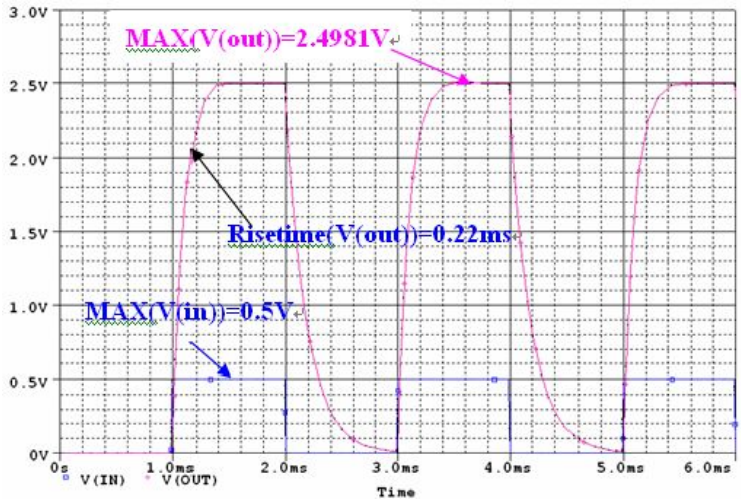

Figure 7. Simulation results of transient response of the current measurement module

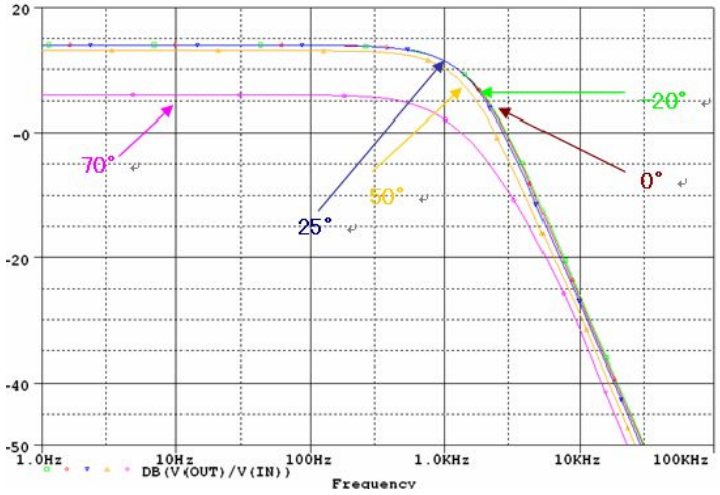

Figure 8. Simulation results under different temperatures of the current measurement module

b. Simulation and analysis of the voltage measurement module

With the same setups, the characteristics of the voltage measurement module are simulated and analyzed as well, and Figure 9 shows the simulation schematic.

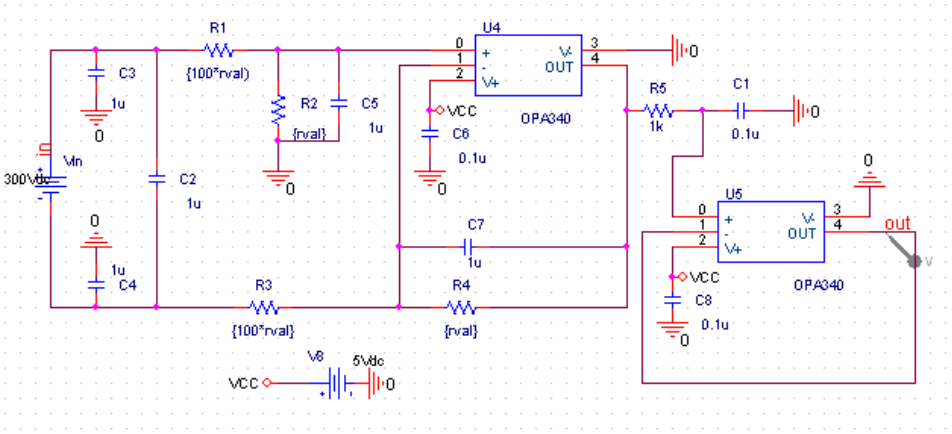

Figure 9. Simulation schematic of the voltage measurement module

The DC output simulation results are “V (OUT)/V_Vin = 9.996E-03, INPUT RESISTANCE AT V_Vin = 2.000E+05 and OUTPUT RESISTANCE AT V (OUT) = 2.877E-02”. Thus the DC error of the voltage sampling is 0.04%. The AC characteristic simulation result is shown in Figure 10, which indicates that the bandwidth is around 1kHz. Figure11 demonstrates simulation results of the transient voltage response, and Figure12 gives out the simulation results of module working under different temperatures, from which we can see that the performance of the module is affected by low temperatures. However, considering the working condition of the real systems, the high temperature rarely exists, so the system can meet the requirements of real applications.

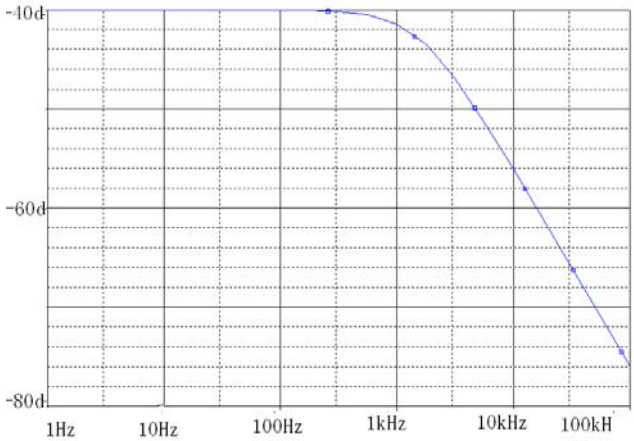

Figure 10. Simulation result of the AC characteristics of the voltage measurement module

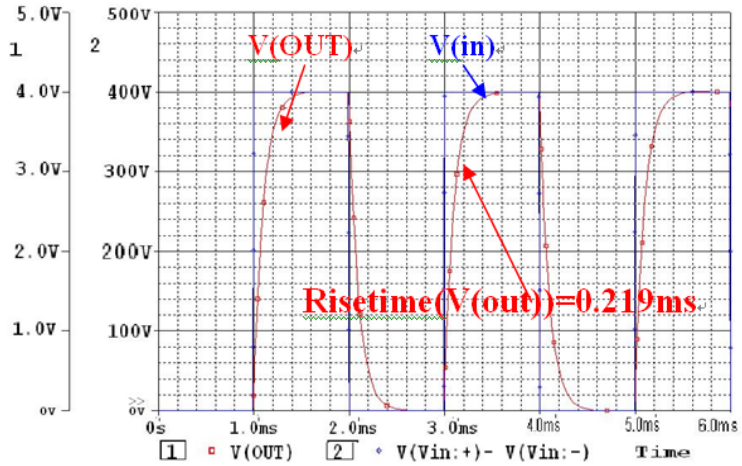

Figure 11. Simulation results of transient response of the voltage measurement module

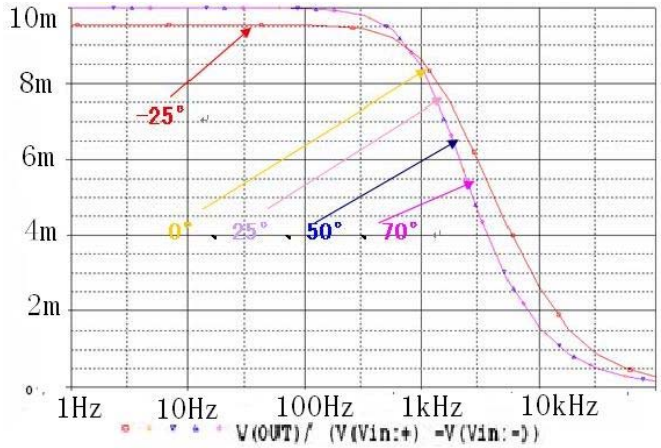

Figure 12. Simulation results under different temperatures of the voltage measurement module

IV. ERROR ANALYSIS AND CORRECTION

a. Error composition analysis

Before going through the acquisition system, the signal carries some noises caused by the environmental interference. This kind of noise can be deemed as random noise. When the signal goes through the acquisition system, it will be converted to the desired signal, meanwhile, the noise is also taking part in the conversion. If the system is non-noise, then, the noise adding on the signal source will be converted by the acquisition system with

$$\Delta y = a \times \Delta x \tag{1}$$

where Δy the converted noise, a the converted function or scaling factor, and Δx the noise in the signal source.

If the system itself bears an error $e\%$, then the noise converted should be

$$\Delta y = a(1+e\%)\times\Delta x \tag{2}$$

This indicates that the signal converted by the acquisition system will be composed of two parts, one is the error scaled by the acquisition system and the other is the system error. So to analyze the error composition of the converted signal, a separate error analysis is needed. Figure 13 shows the error composition of the current measurement module and Figure14 shows the error composition of the voltage measurement module.

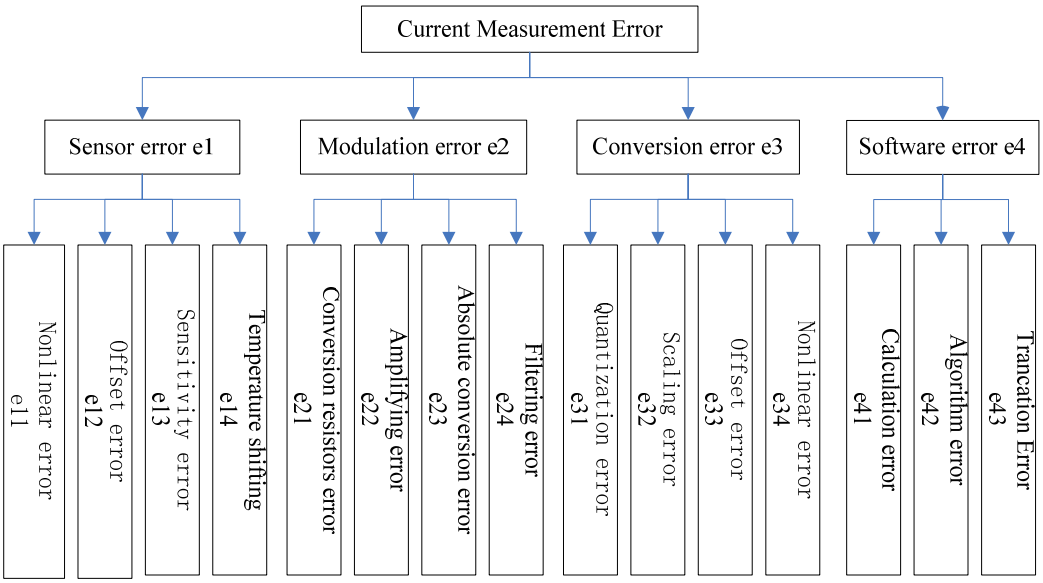

Figure 13. Main error composition of the current measurement module

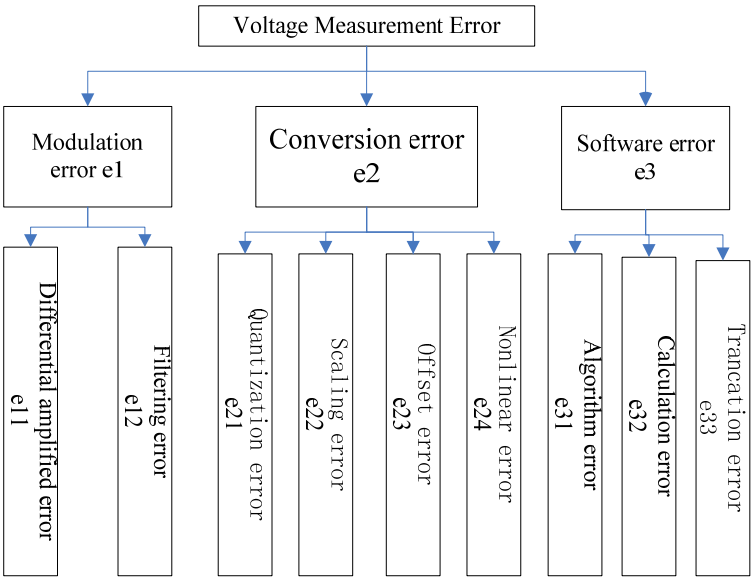

Figure 14. Main error composition of the voltage measurement module

Thus, the error conversion function of the current measurement module is

$$\Delta y = (1+e_1\%)(1+e_2\%)(1+e_3\%)(1+e_4\%)\Delta x \tag{3}$$

and the error conversion function of the current measurement module is

$$\Delta y = (1+e_1\%)(1+e_2\%)(1+e_3\%)\Delta x \tag{4}$$

Although the composition of the error is complex, some improvements can be designed to eliminate or weaken the affects caused by those errors. For example, the error of the sensor, the conversion resistor, the scaling factor of the amplifying circuits, the conversion error of the A/D etc. could be known according to the specification of the system design. Thus, on the one hand, a better hardware design can be considered and on the other hand, a software compensation algorithm can be developed to improve the performance.

b. Theoretical error analysis of voltage measurement module

To the voltage measurement module, the common mode rejection ratio (CMRR) of the operation amplifier is 90dB, thus the *CMRR* of the amplifying circuit is

$$CMRR = \frac{1+Ad}{4k} \tag{5}$$

Where k the resistor factor, and in this study it is 0.0005, Ad the close-loop scaling factor, and it is 100:1 here. With these parameters, the *CMRR* reduces to 54dB.

To evaluate how the offset current affects the performance, the input of the differential circuit can be set to zero, as shown in Figure 15.

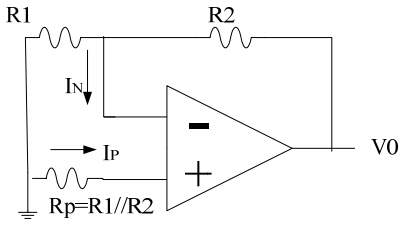

Figure 15. Simplified circuit when analyzing the influence of offset current

If we define the input offset current $I_B = (I_P + I_N)/2$ and $I_{OS} = I_P - I_N$, then

$$V_O = (1 + R2/R1)\{[(R2 // R1) - R_P]I_B - [(R2 // R1) + R_P]I_{OS/2}\} \tag{6}$$

Let *R*p=*R*1//*R*2, then

$$V_O = (1 + R2/R1)(-R2 // R1)I_{OS} \tag{7}$$

According to the specification of the operation amplifier, I_{OS} is $\pm$10pA, so in this system design, the output error caused by input offset current is $\pm$100nV.

When considering the affects caused by input offset voltage V_{OS}, the differential amplifying circuit can be simplified as shown in Figure16, and

$$V_o = (1 + R2/R1)V_{OS} \tag{8}$$

where V_{OS} is influenced by several parameters, as will be discussed below.

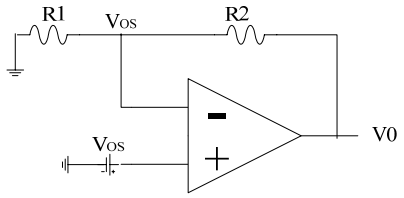

Figure 16. Simplified circuit when analyzing the influence of offset voltage

The V_{OS} is firstly influenced by the temperature, and if the temperature shifting factor is $TC(V_{OS})$, then, the influence can be calculated by

$$\Delta V_{os}(T) = TC(V_{OS}) \times (T - 25°) \tag{9}$$

The common mode rejection ratio affects the V_{OS} in a way like

$$v_o = a(v_P + \frac{v_{CM}}{CMRR} - v_N) \tag{10}$$

Since the CMRR can be adjusted to 90dB, the error caused by common voltage will be neglected. V_{OS} variation caused by the output swing can be calculated by

$$V_{OS} = V_{OS0} + TC(V_{OS})\Delta T + \frac{\Delta v_p}{CMRR} + \frac{\Delta V_S}{PSRR} + \frac{\Delta v_0}{A_{od}} \tag{11}$$

And according to the specifications, the variation caused by output swing is 664uV.

With the principle of superposition,

$$V_O = (1 + R2/R1)[V_{OS} - (R2 // R1)I_{OS}] \tag{12}$$

We can get that V_O(max)=0.7mV, and the relative error δ_1 is 0.02%.

The influence caused by the open-loop scaling factor and CMRR can be calculated by

$$\delta_2 = \frac{1 + \frac{1}{2CMRR}}{1 + \frac{R_1 + R_2}{R_1 A_{od}} - \frac{1}{2CMRR}} - 1 \tag{13}$$

where A_{od} is typically 1e6, then, we can get that the relative error is δ_2=0.0001%, which can obviously be ignored. So the total relative error of the differential amplifying part is $e_{11} = \sqrt{\delta_1^2 + \delta_2^2} \approx \delta_1$=0.02%.

The error caused by the switch capacitor filtering is caused by the filtering components, and the maximum error is e_{12} = 0.02%.

The maximum linear error of the A/D converter is ±6LSB, and the quantization error is 1LSB. With the error synthesize, the error caused by the limited bits is $(\sqrt{6^2 + 1^2} / 2^{16}) \times 100\% = 0.01\%$. Besides, the temperature shifting factor caused a error of ±（0.3ppm/℃×20＋20ppm/℃×20）×100=0.04%. The error caused by the voltage reference is 0.025%. Thus, the synthesized error of the A/D converter is e_{13} = 0.0048%.

So the theoretical error of the voltage measurement module is

$$S_V = \sqrt{e_{11}^2 + e_{12}^2 + e_{13}^2} = 0.056\% \tag{14}$$

c. Theoretical error analysis of current measurement module

With a similar method, the theoretical error of the current measurement module can be attained. One special part is the analysis of the absolute value conversion part.

In this part, when the current is positive, the circuit is actually a follower, so the output error can be got with the specification of the operation amplifier. When the current is negative, the error is caused again by the input offset current, input offset voltage, the power supply rejection ratio (PSRR), the Aod and etc. With a error synthesize, the error caused by this part is 0.04%.

The last theoretical error of the voltage measurement module is $S_{I+} = \sqrt{e1^2 + e2_+^{\ 2} + e3^2} = 0.076\%$, and $S_{I-} = \sqrt{e1^2 + e2_-^{\ 2} + e3^2} = 0.087\%$.

V. VALIDATION TESTING AND DISCUSSIONS

Several testing points are used to validate the performance of the acquisition system. The measured absolute and relative errors under different current are drawn in Figure17.

After getting the absolute error, an error correction algorithm can be developed, which correct the converted signal with the known error, and thereby improves the performance of the system. The errors of the improved system are drawn in Figure 18, from which we can see an obvious performance enhancement, and the maximum absolute error after the correction is 0.05A, the maximum relative error is less than 0.1%.

The absolute error and relative error of the measured voltage are shown in Figure 19, from which we can see that the maximum voltage error of the system is less than 0.06V in all over the voltage range, from 0V to 400V, and the corresponding maximum relative error is less than 0.03%. With a similar method as that in current measurement correction, the measured voltage can be further corrected with a correction algorithm in MCU after the A/D conversion. And the error after correction is shown in Figure 20.

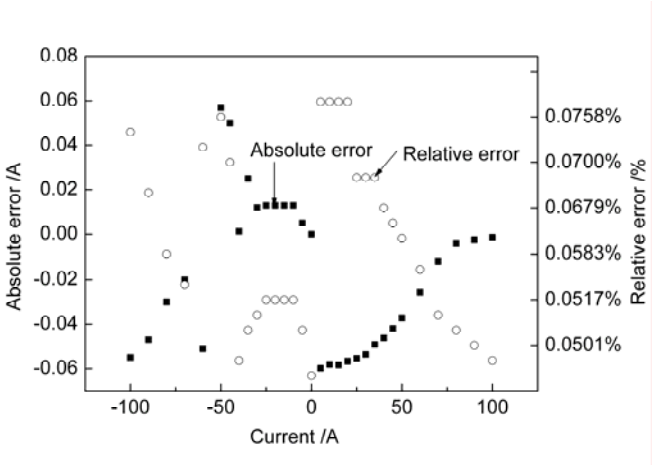

Figure 17. Absolute and relative error of current measurement before correction

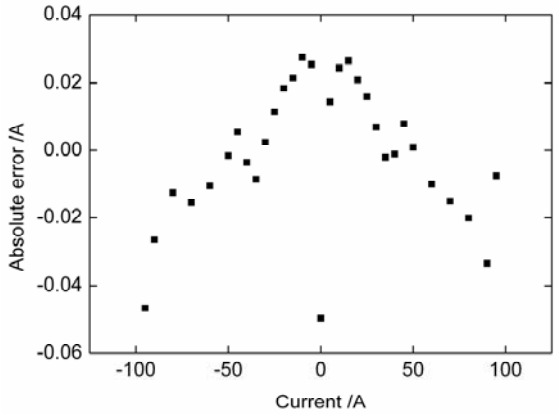

Figure 18. Absolute error of current measurement after correction

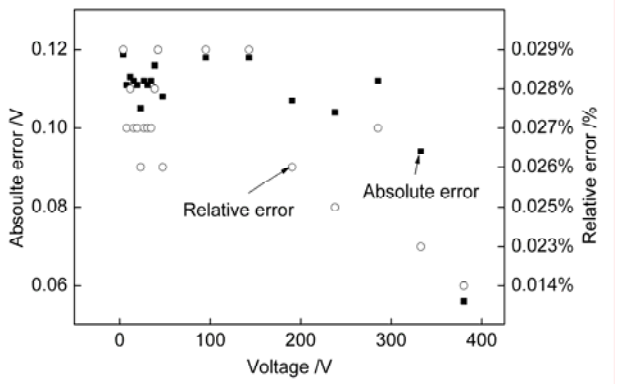

Figure 19. Absolute and relative error of voltage measurement before correction

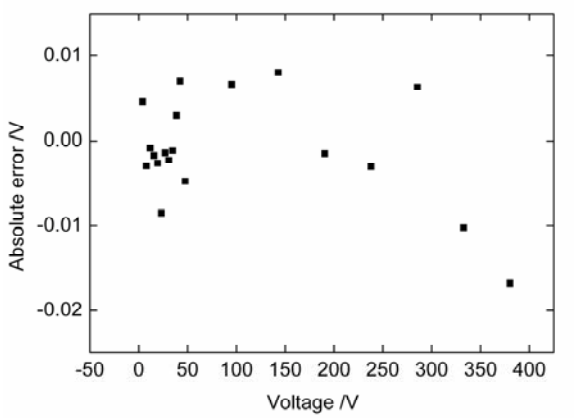

Figure 20. Absolute error of voltage measurement after correction

From Figure 20, we can find that, after the correction, the maximum absolute error is less than 0.02V, and the maximum relative error is less than 0.015%, it outperforms the system before correction.

VI. CONCLUSIONS

This paper presents a detailed design of a current and voltage acquisition system with high accuracy for EV applications. The system includes two main parts, i.e. the current measurement module and the voltage measurement module. A systematic simulation and performance analysis is implemented during the design process. Then, the theoretical errors of the two modules are studied with an error decomposition method. Based on the theoretical errors and the actual measured errors, a correction algorithm has also been developed running in the MCU, which further corrects the signals after the A/D conversion. Several points of tests are designed to evaluate the accuracy of the system. Both current and voltage measurements are very accurate, and the maximum relative error of the current measurement and voltage measurement is 0.1% and 0.015% respectively, which is totally qualified for the EV applications, and guarantees the performance of energy management.

ACKNOWLEDGMENT

This work is financially supported by the National High Technology Research and Development Program (863 Program, Grant No. 2011AA11A265) and the Doctoral Fund of Ministry of Education of China (RFDP, Grant No. 20100072120026).

REFERENCES

[1] Andrew Ford. “The Impacts of Large Scale Use of Electric Vehicles in Southern California”, Energy and Buildings, vol.22, No. 3, 1995, pp. 207-218

[2] Shaik Amjad, S. Nellakrishna and R. Rudramoorthy. “Review of Design Considerations and Technological Challenges for Successful Development and Deployment of Plug-in Hybrid Electric Vehicles”, Renewable and Sustainable Energy Reviews, vol. 14, No. 3, 2010, pp. 1104-1110.

[3] Stephen Brown, David Pyke and Paul Steenhof. “Electric Vehicles: The Role and Importance of Standards in An Emerging Market”, Energy Policy, vol.38, No.7, 2010, pp. 3797-3806.

[4] M.Lieschnegg, B.Lechner, A.Fuchs and O.Mariani. “Versatile Sensor Platform for Autonomous Sensing in Automotive Applications”, International Journal on Smart Sensing and Intelligent Systems, vol.4, No.3, 2011, pp. 496-507

[5] K.T.Chau and Y.S.Wong. “Overview of Power Management in Hybrid Electric Vehicles”, Energy Conversion and Management, vol.43, No.12, 2002, pp.1953-1968.

[6] Yiming He, Mashrur Chowdhury, Pierluigi Pisu and Yongchang Ma. “An Energy Optimization Strategy for Power-split Drivetrain Plug-in Hybrid Electric Vehicles”, Transportation Research Part C: Emerging Technologies, vol.22, June 2012, pp. 29-41.

[7] Sarah J. Gerssen-Gondelach and Andre P.C. Faaij. “Performance of Batteries for Electric Vehicles on Short and Longer Term”, Journal of Power Sources, vol.212, Aug. 2012, pp. 111-129.

[8] Tingting Dong, Xuezhe Wei and Haifeng Dai. “Research on High-precision Data Acquisition and SOC Calibration Method for Power Battery”, Proceeding of IEEE Vehicle Power and Propulsion Conference (VPPC), Sept. 2008, pp. 1-5.

[9] T.Jayakumar, C.Babu Rao, John Philip, C.K.Mukhopadhyay, J.Jayapandian and C.Pandian. “Sensors for Monitoring Components, Systems and Processes”, International Journal on Smart Sensing and Intelligent Systems, vol.3, No.1, 2010, pp. 61-74

[10] Dae-Woong Chung. “Analysis and Compensation of Current Measurement Error in Vector-controlled AC Motor Drives”, IEEE Transaction on Industry Applications, vol. 34, No.2, 1998, pp. 340-345

[11] Hongrae Kim. “Phase Current Reconstruction for AC Motor Drives Using a DC Link Single Current Sensor and Measurement Voltage Vectors”, IEEE Transaction on Power Electronics, vol. 21, No. 5, 2006, pp. 1413-1419

[12] Alex Hakenjos, Harald Muenter, Ursula Wittstadt, Christopher Hebling. “A PEM Fuel Cell for Combined Measurement of Current and Temperature Distribution, and Flow Field Flooding”, Journal of Power Sources, vol. 131, No.1, 2004, pp. 213-216

[13] Jaeger N.A.F, Rahmatian F. “Accurate Voltage Measurement by the Quadrature Method”, IEEE Transactions on Power Delivery, vol. 18, No. 1, 2003, pp. 14-19

[14] Leatherhead. “Method for Simultaneous Measurement of Current and Voltage on High-voltage Lines Using Optical Techniques”, Proceedings of the Institution of Electric Engineers, vol. 123, No.10, 1976, pp. 957-960

[15] Changsheng Li, Toshihiko Yoshino. “Simultaneous Measurement of Current and Voltage by use of One Bismuth Germanate Crystal”, Applied Optics, vol. 41, No. 25, 2002, pp. 5391-5397

[16] Rahmatian F., Jaeger N.A.F. “Accurate Voltage Measurement with Electric Field Sampling Using Permittivity-shielding”, IEEE Transactions on Power Delivery, vol. 7, No.2, 2002, pp. 362-368

[17] Filippov V.N. “Fiber Sensor for Simultaneous Measurement of Voltage and Temperature”, IEEE Photonics Technology Letters, vol. 12, No. 11, 2000, pp. 1543-1545